PRKDC mutations associated with immunodeficiency, granuloma, and autoimmune regulator-dependent autoimmunity

Anne-Laure Mathieu, Estelle Verronese, Gillian I. Rice, Fanny Fouyssac, Yves Bertrand, Capucine Picard, Marie Chansel, Jolan E. Walter, Luigi D. Notarangelo, Manish J. Butte, et al.

HHS Public Access

Author manuscript

J Allergy Clin Immunol. Author manuscript; available in PMC 2015 July 01.

Published in final edited form as:

J Allergy Clin Immunol. 2015 June ; 135(6): 1578–1588.e5. doi:10.1016/j.jaci.2015.01.040.

PRKDC mutations associated with immunodeficiency, granuloma, and autoimmune regulator–dependent autoimmunity

Anne-Laure Mathieu, PhD[a,b,c,d], **Estelle Verronese, BS**[e], **Gillian I. Rice, PhD**[f], **Fanny Fouyssac, MD**[g], **Yves Bertrand, MD, PhD**[h], **Capucine Picard, MD, PhD**[i], **Marie Chansel, MSc**[j], **Jolan E. Walter, MD, PhD**[k], **Luigi D. Notarangelo, MD**[l], **Manish J. Butte, MD, PhD**[m], **Kari Christine Nadeau, MD, PhD**[m], **Krisztian Csomos, PhD**[k], **David J. Chen, PhD**[n], **Karin Chen, MD**[o], **Ana Delgado, BS**[e], **Chantal Rigal, BS**[e], **Christine Bardin, BS**[e], **Catharina Schuetz, MD, PhD**[p], **Despina Moshous, MD, PhD**[j], **Héloïse Reumaux, MD**[q], **François Plenat, MD, PhD**[r], **Alice Phan, MD, PhD**[v], **Marie-Thérèse Zabot, PharmD, PhD**[t], **Brigitte Balme, MD**[s], **Sébastien Viel, PharmD**[a,b,c,d,u], **Jacques Bienvenu, PharmD, PhD**[a,b,c,d,u], **Pierre Cochat, MD, PhD**[v], **Mirjam van der Burg, PhD**[w], **Christophe Caux, PhD**[e], **E. Helen Kemp, BSc, PhD**[x], **Isabelle Rouvet, PharmD, PhD**[t], **Christophe Malcus, PharmD, PhD**[y], **Jean-Francois Méritet, PharmD, PhD**[z], **Annick Lim, MSc**[aa], **Yanick J. Crow, MD, PhD**[f], **Nicole Fabien, PharmD, PhD**[u], **Christine Ménétrier-Caux, PhD**[e], **Jean-Pierre De Villartay, PhD**[j], **Thierry Walzer, PhD**[a,b,c,d], and **Alexandre Belot, MD, PhD**[a,b,c,d,v]

[a]CIRI, International Center for Infectiology Research, Université de Lyon

[b]Inserm U1111, Lyon

[c]Ecole Normale Sup'erieure de Lyon

[d]CNRS, UMR5308, Lyon

[e]Universitée de Lyon, INSERM U1052, Centre de Recherche en Cancérologie de Lyon, Plateforme d'Innovation en Immuno-monitoring et Immunothérapie, Centre Léon Bérard, and in the framework of the LABEX DevWeCan (ANR-10-LABX-0061) of University de Lyon, within the program "Investissements d'Avenir" (ANR-11-IDEX-0007) operated by the French National Research Agency (ANR), Lyon

[f]Manchester Centre for Genomic Medicine, Institute of Human Development, Faculty of Medical and Human Sciences, Manchester Academic Health Centre

[g]Pediatric Haematology and Oncology Department, Children Hospital–CHU NANCY Vandoeuvre les Nancy

[h]Institut d'Hématologie et d'Oncologie Pédiatrique (Hospices Civils de Lyon), Université Claude Bernard Lyon I, Lyon

Corresponding author: Alexandre Belot, MD, PhD, Service de Néphrologie, Rhumatologie, Dermatologie Pédiatriques, Hôpital Femme Mère Enfant, Hospices Civils de Lyon, 57 Bd Pinel, 69677 Bron Cedex, France. alexandre.belot@chu-lyon.fr..

Lyon, Nancy, Paris, and Lille, France, Manchester and Sheffield, United Kingdom, Boston, Mass, Stanford, Calif, Dallas, Tex, Salt Lake City, Utah, Ulm, Germany, and Rotterdam, The Netherlands

Disclosure of potential conflict of interest: The rest of the authors declare that they have no other relevant conflicts of interest.

[i]Study Center for Primary Immunodeficiencies, Assistance Publique-Hôpitaux de Paris, Necker Hospital, Laboratory of Human Genetics of Infectious Diseases, Necker Branch, INSERM U1163, Sorbonne Paris Cité, Paris Descartes University, Imagine Institute, Paris Descartes University, Paris

[j]INSERM UMR 1163, Laboratoire Dynamique du Génome et Systéme Immunitaire Université Paris Descartes–Sorbonne Paris Cité, Imagine Institute, Paris

[k]Pediatric Allergy & Immunology and the Center for Immunology and Inflammatory Diseases, Massachusetts General Hospital, Harvard Medical School, Boston

[l]Division of Immunology, Boston Children's Hospital and Harvard Medical School, Boston

[m]Department of Pediatrics, Division of Immunology, Allergy and Rheumatology, Stanford University

[n]Division of Molecular Radiation Biology Department of Radiation Oncology, University of Texas Southwestern Medical Center, Dallas

[o]Department of Pediatrics, Division of Allergy, Immunology & Rheumatology, University of Utah School of Medicine, Salt Lake City

[p]Department of Pediatrics and Adolescent Medicine, University Medical Center Ulm

[q]Pediatric Rheumatology and Emergency Unit, Jeanne de Flandre Hospital, Lille

[r]Pathology Department, Hémato-Oncologie Pédiatrique, CHU Nancy

[s]Pathology Department, Centre Hospitalier Lyon Sud, Hospices Civils de Lyon

[t]Biotechnology Department, Hospices Civils de Lyon

[u]Immunobiology Department, Hospices Civils de Lyon, Centre Hospitalier Lyon Sud, Lyon

[v]Pediatric Rheumatology, Nephrology and Dermatology Department and EPICIME Hospices Civils de Lyon and Université Claude-Bernard Lyon 1, Lyon

[w]Department of Immunology, Erasmus MC, University Medical Center Rotterdam

[x]Department of Human Metabolism, University of Sheffield

[y]Cell Immunology Department, Hôpital Edouard Herriot, Hospices Civils de Lyon, Lyon

[z]Virology Unit, Hopital Cochin, Assistance Publique-Hôpitaux de Paris

[aa]Immunoscope Group, Immunology Department, Institut Pasteur, Paris

Abstract

Background—*PRKDC* encodes for DNA-dependent protein kinase catalytic subunit (DNA-PKcs), a kinase that forms part of a complex (DNA-dependent protein kinase [DNA-PK]) crucial for DNA double-strand break repair and V(D)J recombination. In mice DNA-PK also interacts with the transcription factor autoimmune regulator (AIRE) to promote central T-cell tolerance.

Objective—We sought to understand the causes of an inflammatory disease with granuloma and autoimmunity associated with decreasing T- and B-cell counts over time that had been diagnosed in 2 unrelated patients.

Methods—Genetic, molecular, and functional analyses were performed to characterize an inflammatory disease evocative of a combined immunodeficiency.

Results—We identified *PRKDC* mutations in both patients. These patients exhibited a defect in DNA double-strand break repair and V(D)J recombination. Whole-blood mRNA analysis revealed a strong interferon signature. On activation, memory T cells displayed a skewed cytokine response typical of T_H2 and T_H1 but not T_H17. Moreover, mutated DNA-PKcs did not promote AIRE-dependent transcription of peripheral tissue antigens *in vitro*. The latter defect correlated *in vivo* with production of anti–calcium-sensing receptor autoantibodies, which are typically found in AIRE-deficient patients. In addition, 9 months after bone marrow transplantation, patient 1 had Hashimoto thyroiditis, suggesting that organ-specific autoimmunity might be linked to nonhematopoietic cells, such as AIRE-expressing thymic epithelial cells.

Conclusion—Deficiency of DNA-PKcs, a key AIRE partner, can present as an inflammatory disease with organ-specific autoimmunity, suggesting a role for DNA-PKcs in regulating autoimmune responses and maintaining AIRE-dependent tolerance in human subjects.

Keywords

Autoimmune regulator; *tolerance*; *DNA-dependent protein kinase catalytic subunit*; PRKDC; *autoimmunity*; *VDJ recombination*; *severe combined immunodeficiency*; *recombination-activating gene*

Severe combined immunodeficiency (SCID) is the most profound phenotype among the primary immunodeficiencies, occurring secondary to mutations in genes affecting lymphocyte development or function.[1] Children with SCID present with high susceptibility to bacterial, viral, and fungal infections in early infancy and are subject to opportunistic infections frequently associated with protracted diarrhea and failure to thrive. In the absence of hematopoietic stem cell transplantation or gene therapy, the disease is usually lethal within the first year of life.

More than 20 different genetic deficiencies have been reported with an SCID phenotype, including genes involved in V(D)J recombination (ie, antigen receptor gene rearrangement [recombination-activating gene 1 *[RAG1]*, *RAG2*, DNA cross-link repair 1C [*DCLRE1C*], *PRKDC*, DNA ligase IV [*LIG4*], and *Cernunnos*]).[2] Typically, patients with SCID have a severe reduction or absence of circulating T cells, and depending on the causative gene, B cells and natural killer (NK) cells might also appear in low numbers or be absent.

Whereas null mutations of SCID-related genes cause typical (classical) SCID, hypomorphic mutations are associated with residual T-cell differentiation and function and result in atypical (leaky) SCID.[2,3] One such well-described phenotype is Omenn syndrome (OS), comprising early-onset generalized erythroderma (before age 1 year), failure to thrive, diarrhea, hepatosplenomegaly, eosinophilia, and increased IgE levels.[4] In most cases of OS, there is residual function of proteins involved in V(D)J recombination.[4,5] Later-onset milder

forms of primary immunodeficiencies can also occur and are characterized by recurrent infections, autoimmunity, and granuloma.[6-8] Interestingly, patients with atypical SCID with a $T^{low}B^{low}$ phenotype were demonstrated to be more prone to immune dysregulation, including development of granuloma, autoimmune cytopenia, and inflammatory bowel disease.[2]

In the context of OS or $T^{low}B^{low}$ SCID (ie, SCID with autoimmunity and granuloma), distinct mechanisms might jointly contribute to the disruption of immune tolerance. First, a break in both central and peripheral B-cell tolerance has been identified in some cases. As an example, in a homozygous *RAG1 S723C* mouse model, V(D)J recombination activity is reduced but not abrogated and is associated with autoantibody production and expansion of immunoglobulin-secreting cells.[9] In this model the efficiency of B-cell receptor (BCR) editing, a mechanism allowing rearrangement of the BCR to reduce its autoreactive specificity, is decreased, and the serum level of B cell–activating factor (BAFF; a key cytokine involved in activation and survival of B cells) is markedly increased.[9]

Second, impaired intrathymic T-cell maturation has been identified. The autoimmune regulator (AIRE) protein is a transcriptional factor expressed in medullary thymic epithelial cells (mTECs), playing a critical role in central T-cell tolerance. AIRE induces ectopic expression of autoantigens in mTECs and drives the negative selection of autoreactive T cells, although the precise molecular mechanisms are still unclear.[10,11] AIRE deficiency leads to the autoimmune polyendocrinopathy, candidiasis, and ectodermal dystrophy (APECED) syndrome[11] and is associated with production of various autoantibodies, including anti–calcium-sensing receptor (CaSR) antibodies in one third of patients.[12] AIRE expression and development of mTECs are dependent on the presence of positively selected T cells.[13-15] A decrease in T-cell production might account for low AIRE expression in the thymus.[16] In patients with OS, *AIRE* mRNA and protein levels are decreased in patients' thymus cells and PBMCs, leading to the suggestion of an impairment in central tolerance.[17] However, no evidence for AIRE-related autoantibodies has been found thus far in these patients.

PRKDC encodes DNA-dependent protein kinase catalytic subunit (DNA-PKcs), which is active when in a heterotrimeric complex (DNA-dependent protein kinase [DNA-PK]) with Ku proteins 70 and 80 and in interaction with DNA or RNA.[18] The main function of DNA-PK is to recognize double-strand DNA breaks and to catalyze a repair process known as nonhomologous end joining. In a similar way DNA-PK is crucial for V(D)J recombination in developing T and B cells. Concordantly, DNA-PKcs or Ku-deficient mice are severely immunodeficient, with increased radiosensitivity and susceptibility to tumor development.[19,20] In addition to its role in DNA recombination, DNA-PK has been recently identified in mice as part of a multiprotein complex required for AIRE-dependent expression of peripheral tissue antigens in mTECs, a process necessary for the establishment of central tolerance.[21]

Previously, 2 unrelated patients with typical SCID were identified, both with mutations in *PRKDC*.[22,23] The patients presented with a $T^{-}B^{-}NK^{+}$ phenotype, failure to thrive, and

chronic infections during the first year of life. One of them also demonstrated growth failure, microcephaly, and seizures.[22]

Here we describe 2 unrelated patients with *PRKDC* mutations presenting with immunodeficiency and autoimmunity. Both patients had granulomas and a variety of autoantibodies. In addition to an oligoclonal T-cell repertoire, these 2 patients exhibited a progressive T- and B-cell deficiency and immune dysregulation with a shift to T_H1 and T_H2, but not T_H17, lymphocytes on activation. We show that *PRKDC* mutations are responsible for a defect of AIRE transcriptional activity *in vitro* and associated with APECED-related autoantibody production.

RESULTS

Clinical features of 2 patients with combined immunodeficiency

This male patient 1 (Pt1) was born to a consanguineous couple of Turkish background (Fig 1, *A*). A younger nonidentical twin brother died in the first year of life with a diagnosis of aspiration pneumonia, chronic diarrhea, and failure to thrive. At birth, Pt1 was unremarkable with normal weight and occipitofrontal head circumference. He was given a diagnosis of persistent asthma in the first 2 years of life and experienced occasional ear infections. At the age of 6 years, he presented with acute arthritis involving the left elbow and right knee with positive antinuclear autoantibody (ANA) levels (Fig 1, *B*), which is indicative of oligoarticular juvenile idiopathic arthritis. He responded well to intra-articular steroid injections and methotrexate. However, after poor methotrexate tolerance (recurrent pneumopathy), this treatment was discontinued. At the 8 years of age, he was given a diagnosis of bronchiectasis, splenic granuloma (Fig 1, C), and skin granuloma (Fig 1, *D* and *E*). Periodic acid–Schiff and Ziehl-Neelsen staining revealed no pathogens (data not shown). PCR assays for *Mycobacteria* species and 16s RNA were negative, and a diagnosis of sarcoidosis was suggested. Initial T- and B-cell counts were normal, with increased serum immunoglobulin levels (Table I). Over time, immunoglobulin subclass assessment revealed a deficiency in IgA, IgG_2, and IgG_4. A decrease in T- and B-cell numbers was also observed, whereas NK cells remained within the normal range. Strikingly, memory phenotype $CD4^+CD45RO^+$ T cells represented more than 90% of circulating CD4 T cells, and $CD4^+CD45RA^+$ T cells were decreased to less than 5%. Immunoglobulin subclass analysis revealed a deficiency in IgA, IgG_2, and IgG_4, whereas total IgG levels were increased. Maternal engraftment of T cells was ruled out by using PCR (data not shown), and a diagnosis of combined immunodeficiency (CID) with autoimmunity and granuloma was made.

After myeloablative conditioning with fludarabine and busulfan, Pt1 underwent bone marrow transplantation (BMT) from his HLA-identical mother, which resulted in reconstitution with 100% donor chimerism of the myeloid, B-cell, and T-cell compartments. Nine months after transplantation, his skin granuloma had disappeared. However, concomitant with donor T-cell expansion, symptomatic Hashimoto thyroiditis appeared with fatigue, sensitivity to cold, low cardiac rate, and increased thyroid-stimulating hormone, positive anti-thyroid peroxidase (>300 IU/mL), and anti-thyroglobulin (>3000 IU/mL) antibody levels. Thyroxin substitution was started.

An unrelated female patient (Pt2) was born to a nonconsanguineous couple of Turkish background (Fig 1, *F*). Familial history revealed 4 deaths in the first 2 years of life attributed to prematurity (II.4 and II.5) or sepsis (II.6 and II.7). She presented with a history of recurrent lung infections. Bronchiectasis was recognized at the age of 5 years, and splenic granulomatous lesions were identified at 9 years of age on an abdominal computed tomographic scan (Fig 1, *G*). Splenic biopsy specimens revealed well-circumscribed caseating epithelioid granulomas with negative special stains for microorganisms (Fig 1, *H*). At the age of 20 years, she had symmetric polyarthritis (elbow and knee) sensitive to nonsteroidal anti-inflammatory drugs. Immunologic assessment revealed low numbers of circulating T and B cells and normal T-cell proliferation with mitogen and antigens (Table I). IgG levels were increased to greater than 22 g/L, with a monoclonal gammopathy (IgG_{2k2}), even though circulating B cells were undetectable. NK cell counts were normal, defining $T^{low}B^{-}NK^{+}$ CID. ANAs were also detected in the serum of Pt2.

PRKDC mutations are present in both patients with CID

Mutations in *RAG1* and *RAG2* were excluded by means of Sanger sequencing. A homozygous locus encompassing *PRKDC* was identified on chromosome 8 by using single nucleotide polymorphism analysis in Pt1 and predicting an autosomal recessive pattern of inheritance. Sanger sequencing identified a c.9185T>G (p.Leu3062Arg) homozygous missense variant and a homozygous c.6340delGAG (pGly2113del) deletion in *PRKDC* in this patient (Fig 1, *I*). The glycine deletion has an allele frequency of 1% (rs79703138) and has previously been determined as likely nonpathogenic.[23] Conversely, the c9185T>G homozygous variant was predicted as pathogenic on the basis of species conservation, the output of pathogenicity prediction packages (SIFT: deleterious/score, 0; POLYPHEN: probably damaging/score, 1), and their absence from the dbSNP and 1000 Genomes project databases and 13,006 control chromosomes typed for this allele on the Exome Variant Server. One previous report demonstrated that the c9185T>G variant results in decreased Artemis activation, leading to impaired coding joint formation and a defect in recombination.[23] The parents of Pt1 were heterozygous for the 2 variants. Sequencing of the unrelated patient Pt2 revealed the same 2 variants in the homozygous state.

Patients' fibroblasts are defective in DNA double-strand break repair

Previously, *PRKDC* mutations have been associated with a defect in DNA double-strand break (DSB) repair.[22,23] We first assessed cell survival after 7 days of treatment with the radiomimetic drug phleomycin. Primary fibroblasts of both patients displayed a dose-dependent defect in survival compared with control fibroblasts. Their survival was similar to that of radiosensitive CERNUNNOS-deficient cells at a dose of 400 ng/mL phleomycin (Fig 2, *A*). Therefore we analyzed the DSB repair defect in more detail by counting foci of the DSB marker 53BP1 after irradiation in Pt2's fibroblasts. 53BP1 foci remained increased at 24 hours compared with the control (Fig 2, *B*, and see Fig E1 in this article's Online Repository at www.jacionline.org). Thus we confirmed earlier findings that cells with *PRKDC* mutations result in defective DNA DSB repair.[23]

The T-cell receptor Vβ repertoire is limited in patients with *PRKDC* mutations

DNA-PKcs is mandatory for V(D)J recombination in mice, and the 2 previously described patients with *PRKDC* mutations demonstrated a complete lack of T and B cells.[22,23] By contrast, the 2 patients reported here presented with circulating T and B cells. Therefore we investigated the T-cell Vβ repertoire in both patients using flow cytometry (18 Vβ families with anomalies in Pt1 and Pt2; Fig 2, *C*) and quantitative PCR (276 combinations Vb-J, IMGT nomenclature, in Pt1; Fig 2, *D*) at different time points. Molecular PCR analysis of TRBV-J combinations revealed a poorly diversified peripheral T-cell repertoire in Pt1 (Fig 2, *D*), together with commonly overrepresented rearrangements, such as TRB V27-J2.3, V19-J2.1, V07-J2.1, V10-J1.4, V07-J2.7, V02-J2.2, V03-J1.3, and V05-J2.7. In Pt2 $V\beta29^+$ T cells were clonally expanded, whereas most other Vβ families in both patients were underrepresented. These data are consistent with limited V(D)J recombination in both patients. We used Immunoscope technology to analyze the T-cell repertoire of Pt2 (Fig 2, *E*). The latter experiment showed a major oligoclonal expansion of Vβ29 T cells.

Patients with *PRKDC* mutations have increased BAFF levels and numbers of inflammatory monocytes and memory T cells expressing T_H1 and T_H2, but not T_H17, cytokines on activation

Limited data are available on the distribution and function of residual T cells in patients with CID with autoimmunity and granuloma. T_H1 cytokines, T_H17 cytokines, or both are supposed to promote granuloma formation.[24] In both patients we first explored the expression of and response to cytokines in the blood. The expression of 6 interferon-stimulated genes (*IFI27*, *IFI44L*, *IFIT1*, *ISG15*, *RSAD2*, and *SIGLEC1*) was strongly increased in both patients, thus indicating potent *in vivo* interferon induction (Fig 3, *A*). In addition, the expression of BAFF, TNF-α, and IFN-γ mRNA in both patients was upregulated in whole blood cells, similar to that seen in patients with *IFIH1* mutations, a recently identified cause of interferon-driven autoimmunity (Fig 3, *B*).[25] In contrast, IL-17A and IL-6 transcripts remained within the normal range (see Fig E2, *A*, in this article's Online Repository at www.jacionline.org). Consistent with these quantitative PCR data, high BAFF and TNF-α levels were detected in the sera of Pt1 and Pt2 compared with those in control subjects (Fig 3, C). After BMT, BAFF levels decreased in Pt1 to those of a patient with a hypomorphic mutation in Artemis (see Fig E2, *B*). IFN-γ levels were normal in the patient's sera. Type I interferon activity, as measured by using a viral cytopathic assay, was also found to be normal in the serum of Pt2 (data not shown).

Next, we analyzed the frequency of a wide range of immune cell subsets in whole blood using flow cytometry and assessed intracellular expression of several cytokines in lymphocytes on stimulation with phorbol 12-myristate 13-acetate (PMA)/ionomycin (Fig 3, *D-H*, and Table I). The percentage of NK and dendritic cells appeared normal in both patients. An increased number of inflammatory $CD14^+CD16^+$ monocytes was detected in patients compared with age-matched control subjects. $CD4^+$ and $CD8^+$ naive T-cell counts were dramatically reduced in patients, which is in line with a low thymic output. Interestingly, most $CD4^+CD45RA^+$ T cells, which are routinely referred to as naive T cells, were actually memory T cells with no CCR7 expression, defining the T effector memory with RA^+ (TEMRA) subset (data not shown). Similarly, patients' $CD4^+CD39^+$ regulatory T

cells did not express CD45RA, suggesting a defect in the thymic development of natural regulatory T cells (see Fig E2, *C*). On stimulation with PMA and ionomycin (5 hours' treatment), the production of T_H1-related (IFN-γ and TNF-α), T_H2-related (IL-4 and IL-13), or T_H17-related (IL-17A) cytokines by blood T-cell subsets was measured by using intracellular staining (Fig 3, *D-H*). Interestingly, $CD4^+$ and $CD8^+CD45RA^-$ memory T cells of both patients secreted more T_H2 cytokines (IL-4 and IL-13) than those of control subjects, an observation already reported in patients with OS (Fig 3, *F* and *G*). The T_H1 cytokines TNF-α and IFN-γ were induced in memory T cells (no difference compared with control subjects), whereas IL-17A expression was reduced in $CD45RA^-$ T cells, suggesting that T_H17 cells do not play a role in the pathogenesis of autoimmunity and granuloma in patients with *PRKDC* mutations (Fig 3, *H*).

AIRE-dependent peripheral tissue antigen expression is impaired by *PRKDC* mutations

Recently, in mice DNA-PK was identified as a direct molecular partner of AIRE in the thymus,[21] collaborating with AIRE to induce peripheral tissue antigen transcription by mTECs. Therefore we hypothesized that *PRKDC* dysfunction might impair the ability of DNA-PK to promote AIRE transcriptional activity. To test this hypothesis, we analyzed fibroblasts derived from control subjects, from Pt1 and Pt2, and from a patient displaying a typical SCID phenotype (Pt3) previously reported with the same *PRKDC* mutations.[23] Fibroblasts were transiently transfected with *AIRE* cDNA. In wild-type human fibroblasts we measured the expression of AIRE-dependent (*IGFL1*, *ALox12*, and *S100A8*) and AIRE-independent (*PRMT3*, *CCNH*, and *CXCL10*) transcripts, as identified by Abramson and colleagues,[21] by using quantitative PCR after confirming that AIRE was expressed in fibroblasts by using Western blotting (Fig 4, *A*). Expression of *PRMT3*, *CCNH*, and *CXCL10* was not modified after AIRE transfection in fibroblasts (Fig 4, *A*), whereas *IGFL1* was strongly increased by 60-fold in wild-type fibroblasts. In contrast, *AIRE*-transfected fibroblasts from Pt1 and Pt2 had reduced induction of *IGFL1* in comparison with that in control subjects (Fig 4, *B*). Similar results were obtained with *AIRE*-transfected fibroblasts from the previously reported patients with SCID (Pt3; Fig 4, *C*). After *AIRE* transfection, S100A8 expression was induced in control fibroblasts but not in fibroblasts of patients with *PRKDC* mutations (data not shown). Taken together, these data indicate that mutated DNA-PKcs prevent AIRE-dependent transcription.

Patients have positive autoantibody responses against the CaSR

Because the impairment of AIRE function can lead to autoimmune responses against peripheral tissue antigens, we characterized the pattern of autoantibodies in Pt1 and Pt2. In addition to ANAs, both patients had positive anti-CaSR autoantibody levels (Fig 4, *D* and *E*). However, other tissue-specific autoantibodies (tyrosine hydroxylase, phenylanine hydroxylase, tryptophan hydroxylase, and NALP5) and anti-cytokine autoantibodies (IFN-α2A, IFN-ω, IFN-λ1, IL-22, IL-17A, and IL-17F) were not detected (data not shown). Anti-CaSR autoantibodies are found at a high prevalence in patients with APECED.[10,12,21] Importantly, 7 additional patients with atypical SCID with defective V(D)J recombination, granuloma, and autoimmunity who did not have *PRKDC* mutations had negative anti-CaSR autoantibody levels (Table II). This suggests that the anti-CaSR autoantibody response is specific to the DNA-PK defect found in Pt1 and Pt2. After BMT of Pt1, anti-CaSR

autoantibody levels strongly decreased, although immunoblotting demonstrated slight persistent positivity (Fig 4, *D*), and Hashimoto thyroiditis occurred 9 months after BMT with the appearance of donor T and B cells (Fig 4, *E*).

DISCUSSION

Extending the phenotype of patients with *PRKDC* mutations, we report here the cases of 2 unrelated patients with manifestations of CID with immunodeficiency, granuloma, and autoimmunity caused by a homozygous p.Leu3062Arg mutation in *PRKDC*. Recurrent infections were documented in both cases, but their clinical history did not reveal opportunistic infections. Inflammatory manifestations were prominent in Pt1, who was initially given a diagnosis of ANA-positive oligoarticular juvenile idiopathic arthritis. He subsequently had skin granuloma and lung involvement, which was considered indicative of sarcoidosis. Pt2 was given a diagnosis of a CID at the age of 9 years. There was no obvious neurological involvement in either patient. Pt2 had 2 healthy children.

Both patients carried the same homozygous pathogenic p.Leu3062Arg variant as the first patient published with a mutation in *PRKDC*.[23] All 3 patients shared a common Turkish ancestry, suggesting a founder effect for these variants. The first 2 patients reported with *PRKDC* mutations presented with a typical SCID phenotype, including recurrent candidiasis and lower pulmonary infections. Of note, 1 sibling of Pt1 and 4 siblings of Pt2 died early in life from recurrent infections. We did not have access to DNA for these subjects, but we speculate that their deaths were related to the same primary immunodeficiency being responsible for typical SCID. The range of clinical phenotypes strongly suggests that additional factors contribute to the overall severity of the disease. Stochastic events or other modifying genes might affect the overall manifestation of this deficiency. This is reminiscent of the situation already described for T^-B^- SCID and OS within the same family harboring the same *RAG1* mutation.[26]

The hallmark of classical OS is an expansion of autoreactive T cells with an HLA-$DR^+CD45RO^+$ phenotype and an oligoclonal T-cell repertoire.[4] In patients with OS, the response of activated T cells is skewed toward a T_H2 type and is associated with increased secretion of IL-4 and IL-5, which is responsible for an increased production of IgE and eosinophilia, respectively.[27] Here, in the 2 patients with *PRKDC* mutations, production of T_H2 cytokines was also slightly increased in memory T cells on stimulation. T_H1 and T_H17 cells are recognized to play pivotal roles in autoimmunity and granuloma formation in patients with various inflammatory conditions, such as Crohn disease, juvenile idiopathic arthritis, and sarcoidosis.[28-30] Both protein and mRNA levels of the T_H1 cytokines IFN-γ and TNF-α were increased in serum and whole blood cell transcripts as well as on stimulation of memory T cells isolated from both patients with CID (similar to levels in control subjects). However, on activation, T_H17 cytokine levels were reduced in memory T cells. We hypothesize that T_H1 and T_H2 cytokines can drive immunopathology in patients with CID with granuloma and autoimmunity. Unexpectedly, however, neither IFN-γ nor type-I interferon activity was measureable in Pt2's serum, whereas whole blood cells displayed a strong interferon signature. This signature might be acquired after intratissular activation of T cells or might be secondary to chronic activation of innate pathways in

response to environmental antigens.[31] Furthermore, BAFF levels were increased in both DNA-PKcs–deficient and ARTEMIS-deficient patients, as reported in patients with hypomorphic RAG,[9] and might promote autoreactive B-cell survival. Interestingly, BAFF is produced by activated monocytes and also promotes T_H1-associated inflammation in mice. BAFF and T_H1 cytokines might synergize in patients with CID and lead to autoimmunity.[32,33]

In the context of a recombination defect, there are several overlapping mechanisms, as detailed in the introduction, which might lead to autoimmunity. ANA^+ arthritis has been identified in other patients with immunodeficiency[34,35] and might be related to the T- and B-cell developmental defect, impaired BCR editing, repertoire disruption, and immune cell cytokine overproduction (eg, TNF-α and BAFF in Pt1 and Pt2). We think that in the context of *PRKDC* mutation, one additional mechanism should be considered: direct impairment of AIRE-dependent tissue-specific antigen expression could promote APECED-like manifestations. The relevance of interactions between AIRE, which plays a critical role in the negative selection of autoreactive T cells,[10,11] and DNA-PK was previously tested by using NOD.CB17-$Prkdc^{scid}$ mice, which have an inactive form of DNA-PK.[21] These mice lack mature thymocytes and therefore mTECs, which depend on thymocyte crosstalk for maturation.[23-26] Mice were reconstituted with wild-type bone marrow to generate chimeric animals with wild-type lymphocytes and DNA-PK mutant mTECs to circumvent this issue. Reconstituted NOD.CB17-$Prkdc^{scid}$ mice, but not control mice, demonstrated reduced transcription of AIRE-dependent genes in mTECs, despite similar levels of AIRE expression. The mice also had late-onset autoimmunity characterized by autoantibody production. Overall, the results indicated that DNA-PK expression in mTECs is crucial to AIRE function.[21]

In the context of *PRKDC* mutations, we have shown that AIRE transcriptional activity is directly impaired, leading to a decrease in (eg, IGFL-1), or absence of (eg, S100A8) expression of AIRE-dependent peripheral tissue antigens. These findings are associated with *in vivo* production of anti-CaSR autoantibodies, which were absent in 5 patients with atypical SCID with hypomorphic *RAG* mutations and 1 with *DLCRE1C* (ARTEMIS) mutation with granuloma and autoimmunity. Moreover, Pt1 had Hashimoto thyroiditis 9 months after transplantation, which is a rare event in the course of BMT but can be sometimes observed. Positivity of glutamic acid decarboxylase (GAD) antibodies is also uncommon. These organ-specific autoantibodies suggests that mTECs, which are not replaced on BMT, promoted autoimmunity mediated by newly emigrant naive T cells. Anti-CaSR autoantibody levels were also slightly positive after BMT in the same patient, which might also reflect the persistence of central tolerance defect. Two other patients have been reported with *PRKDC* mutations and an SCID phenotype with a complete absence of T and B cells but no autoimmune manifestations. We acknowledge also that the organ-specific autoimmunity observed in our patients could be unrelated to the *PRKDC* mutation. One can also speculate that few circulating T cells, B cells, or both are mandatory for the development of such autoimmune features. After BMTof the previously reported patient with SCID (Pt3), the last examination did not reveal autoimmune signs. This suggests that the penetrance of AIRE-associated autoimmunity could be incomplete.

In summary, *PRKDC* mutations in human subjects can mimic inflammatory disease with autoimmunity and granuloma. In the patients with CID described here, increased cytokine expression might contribute to autoimmunity and granuloma. In addition, *PRKDC* hypomorphic mutations prevent AIRE function. Organ-specific autoimmunity might result from the defective interaction of mutated DNA-PKcs and AIRE in the thymus, and anti-CaSR might serve as potential biomarker of this condition.

METHODS

Immunohistochemical analyses

Morphological studies of skin and spleen biopsy specimens were carried out on 5-μm-thick, formalin-fixed, paraffin-embedded samples with hematoxylin and eosin staining.

Clonogenic survival assays

Fibroblasts (10^4) from a healthy control subject, a Cernunnos-deficient patient, or Pt1 and Pt2 were plated in duplicates on day 0 in culture medium. Increasing doses of the radiomimetic drug phleomycin (InvivoGen, Toulouse, France) was added, and cells were cultured for 7 days. We measured cell numbers by using flow cytometry and analyzed the percentage of surviving cells as the ratio of treated/untreated cells.

Analysis of 53BP1 foci after ionizing radiation

Early passaged primary fibroblasts were cultured on cover slips and X-irradiated (5 Gy). One or 24 hours after irradiation, cells were washed with PBS, fixed with 4% paraformaldehyde for 15 minutes, and incubated for 20 minutes with PBS/0.1 mol/L glycine. Cells were then permeabilized in 0.5% Triton X-100 in PBS for 15 minutes. After each step, cover slips were rinsed 3 times with PBS. Thereafter, cells were incubated for 30 minutes with PBS-BSA 1% and labeled (30 minutes) with primary antibodies (Anti-53BP1; Novus Biological, Littleton, Colo). Then cells were washed with PBS/BSA 1% solution and incubated (30 minutes) with secondary antibodies (Alexa Fluor 488 goat $F[Ab']_2$; Molecular Probes, Eugen, Ore). Slides were stained for 5 minutes with 0.1 μg/mL 4′-6-diamidino-2-phenylindole dihydrochloride and mounted in FluorSave (Calbiochem, Nottingham, United Kingdom). Slides were analyzed by using epifluorescence microscopy (Axioplan; Zeiss, Oberkochen, Germany). Images were processed for quantification with ImageJ software.

T-cell receptor Vb repertoire analysis

T-cell repertoire diversity was measured with the Human ImmunTraCkeR test (ImmunID Technologies), a technology based on genomic DNA Multi-N-plex quantitative PCR technology.[E1] Human T-cell receptor Vβ-J rearrangements were documented according to IMGT nomenclature (www.imgt.org). Phenotypic analysis of the T-cell Vb repertoire was performed on whole blood samples by using the IOTest Beta Mark kit (Beckman Coulter, Villepinte, France) containing 24 mAbs identifying approximately 70% of the T-cell repertoire. Whole blood cells were stained with PECy5-conjugated CD3, PECy7-conjugated CD4, and each combination of 3 fluorescein isothiocyanate–, phycoerythrin-, and fluorescein isothiocyanate/phycoerythrin-conjugated anti-Vb mAbs in 8 sample tubes. Whole blood samples were automatically lysed with the IMMUNOPREP Reagent System

(Beckman Coulter), washed, and fixed in 0.5% formaldehyde in PBS. T cells (0.5 to 1 × 10^4) were acquired on a Cytomics FC500 flow cytometer, and data were analyzed with CXP analysis software. All reagents and instruments were purchased from Beckman Coulter. Lymphocytes were first gated according to forward-scatter/side-scatter parameters, and then $CD3^+$, $CD4^+$, and $CD3^+CD4^-$ cells were selected. The proportion of each Vb family was compared with the minimum and maximum of each reference value obtained from IOTest Beta Mark kit–related data to evaluate expanded or restricted Vb families. Expansions or restrictions were defined respectively for values greater than the maximum or less than the minimum reference values of the corresponding family.

Immunoscope quantitative repertoire

The methods have been described elsewhere.[E2] Briefly, the total RNA Miniprep Kit (Qiagen, Courtaboeuf, France) was used, and cDNA was synthesized with SuperScript II Reverse Transcriptase (Invitrogen by Life Technologies, Carlsbad, Calif). PCR reactions were carried out by combining a reverse primer and a specific fluorophore-labeled probe for the constant region (MGB–TaqMan probe) with 1 of 24 primers covering the different TRBV chains. The different human TRBV germline genes can be clustered in 24 families according to their level of homology (IMGT nomenclature). Real-time PCR reactions were subsequently carried out with a final concentration of 400 nmol/L of each oligonucleotide primer, 200 nmol/L of the fluorogenic probe, and FastStart Universal Probe Master Rox (Roche, Mannheim, Germany). Thermal cycling conditions comprised TaqDNA Polymerase activation at 95°c for 10 minutes and then subjected to 40 cycles of denaturation at 95°c for 15 seconds, annealing, and extension at 60°c for 1 minutes. For all these reactions, real-time quantitative PCR was then performed on an ABI-7300 system (Applied Biosystems by Life Technologies, Carlsbad, Calif). The relative use of each TRBV family was calculated according to the following formula:

$$\mathrm{U\,(BVy)} \quad = \quad \sum_{x\ =\ 1}^{x\ =\ 24} 2^{(Ct(\mathrm{x})-Ct(\mathrm{y}))},$$

where *Ct(x)* is the fluorescent threshold cycle number measured for the BVy family.

For Immunoscope profiles, products were then subjected to run-off reactions with a nested fluorescent primer specific for the constant region for a total of 3 cycles. The fluorescent products were separated and analyzed with an ABI-PRISM 3730 DNA analyzer. The size and intensity of each band were analyzed with Immunoscope software,[E3] which has been adapted to the capillary sequencer. Fluorescence intensities were plotted in arbitrary units on the y-axis, and CDR3 lengths (in amino acids) were plotted on the x-axis.

Measurement of whole blood cytokine expression

Blood was collected into PAXgene tubes (PreAnalytix, Hombrechtikon, Switzerland) and, after being kept at room temperature for between 2 and 72 hours, was frozen at −20°C until extraction. Total RNA was extracted from whole blood with a PAXgene (PreAnalytix. Hombrechtikon, Switzerland) RNA isolation kit. RNA concentration was assessed with a

spectrophotometer (FLUOstar Omega; Labtech, Ortenberg, Germany). Quantitative RT-PCR analysis was performed with the TaqMan Universal PCR Master Mix (Applied Biosystems, Paisley, United Kingdom) and a cDNA derived from 40 ng of total RNA. TaqMan probes were used for *IFI27* (Hs01086370_m1), *IFI44L* (Hs00199115_m1), *IFIT1* (Hs00356631_g1), *ISG15* (Hs00192713_m1), *RSAD2* (Hs01057264_m1), *SIGLEC1* (Hs00988063_m1), *IL1B* (Hs01555410_m1), *IL6* (Hs00985639_m1), *TNFA* (Hs99999043_m1), *IFNG* (Hs00989291_m1), *IL17A* (Hs00174383_m1), and *TNFSF13* (BAFF; Hs00198106_m1). The relative abundance of each target transcript was normalized to the expression level of *HPRT1* (Hs03929096_g1) and *18S* (Hs999999001_s1) and assessed with the Applied Biosystems StepOne software (version 2.1) and DataAssist software (version 3.01). For each of the 6 probes, individual (patient and control) data were expressed relative to a single calibrator (control C25). The relative quantification for each transcript is equal to $2^{-\Delta Ct}$ (ie, the normalized fold change relative to a control).

BAFF ELISA

BAFF levels were measured in serum samples with a Human BAFF/BLyS/TNFSF13B Quantikine ELISA Kit (R&D Systems, Minneapolis, Minn), according to the manufacturer's protocol. The BAFF concentration was recorded in picograms per milliliter.

TNF-α, IFN-γ, and type I interferon

IFN-γ and TNF-α levels were measured with an ELISA kits (Life Technologies), according to the manufacturer's instructions. IFN-γ and TNF-α concentrations were recorded as international units per milliliter and picograms per milliliter, respectively. IFN-α is titrated by using the cytopathic effect inhibition assay, as previously described.[E4] In this antiviral assay about 1 U/mL interferon is the quantity necessary to produce a cytopathic effect of 50%. Interferon activity is measured on bovine MDBK cells with vesicular stomatitis virus.[E5] Units are determined with respect to the World Health Organization international standard for Hu-IFN-Alpha 2b (code 95/566) provided by the National Institute for Biological Standards and Control (Pestka 1986).

Phenotypic analysis on whole blood cells

Briefly, 0.5 to 1×10^6 whole blood cells were stained with a mixture of fluorochrome-labeled antibodies for each panel for 20 minutes at 4°C and then washed twice in staining buffer (PBS, 2% FBS, and 1 mmol/L EDTA). Erythrocytes were lysed at room temperature for 10 minutes in the dark with BD Pharm Lyse buffer 1X (BD Biosciences, Le Pont de Claix, France). Cells were resuspended in 300 mL of staining buffer in the presence of 2 μL of 4′-6-diamidino-2-phenylindole dihydrochloride (2 μg/mL) to exclude dead cells, and all events were acquired on a FACSCanto II flow cytometer (BD Biosciences). Results were analyzed with FlowJo software, version 9.6.4 (TreeStar, Ashland, Ore). Monocytes were identified as classical ($CD14^+CD16^-$), activated ($CD14^+CD16^+$), or nonclassical ($CD14^-CD16^+$). CD4 T cells were identified as naive ($CD3^+CD4^+$ $CD45RA^+CCR7^+$), central memory (TCM; $CD3^+CD4^+CD45RA^-CCR7^+$), effector memory RA1 ($CD3^+CD4^+CD45RA^+CCR7^-$), or effector memory (TEM; $CD3^+CD4^+CD45RA^-CCR7^-$). CD8 T cells were identified as naive ($CD3^+CD4^-CD45RA^+CCR7^+$), central memory

(TCM; $CD3^+CD4^-$ $CD45RA^-CCR7^+$), effector memory RA1 (TEMRA; $CD3^+CD4^-$ $CD45RA^+CCR7^-$), and CD8 effector memory (TEM; $CD3^+CD4^-CD45$ RA^-CCR7^-).

Assessment of cytokine production in activated whole blood cells

Briefly, 900 μL of heparinized whole blood was incubated at 37°C in a 5% CO_2 humidified atmosphere for 5 hours in the presence or absence of PMA (50 ng; Sigma-Aldrich, Saint Quentin Fallavier, France) and ionomycin (1 ng/mL, Sigma-Aldrich) together with a protein transport inhibitor (GolgiPlug, 10 μg/mL, BD Biosciences). At the end of stimulation, erythrocytes were lysed at room temperature with BD Pharm Lyse buffer. White blood cells were washed in staining buffer and stained with the corresponding surface antibodies panel. After washing in PBS, cells were fixed with formaldehyde (Sigma-Aldrich) at 2% for 20 minutes at 4°C, washed twice in staining buffer, and stored overnight at 4°C. Cells were then permeabilized in staining buffer supplemented with 0.5% saponin and stained for 20 minutes at 4°C with the corresponding intracytoplasmic anti-cytokine antibodies (IL-2, IL-4, IL-13, IL-17, IFN-γ, and TNF-α). Cells were resuspended in 600 μL of staining buffer, and all events were acquired on a flow cytometer fitted with 4 lasers (violet, blue, yellow, and red; LSRII Fortessa for functional analyses BD biosciences). Results were analyzed with FlowJo software, version 9.6.4, and cytokine secretion by different cell subsets defined by the gating strategy was evaluated by creation of Boolean gates.

Fibroblast transfection and immunoblotting to detect AIRE expression

Primary fibroblasts were cultured from a skin biopsy sample from Pt1, Pt2, or a control subject in Dulbecco modified Eagle medium supplemented with 10% FBS, 2 mmol/L glutamine, 10 mmol/L HEPES, and 40 μg/mL gentamicin (Life Technologies, Courtaboeuf, France). Fibroblasts were transfected with either pMax-GFP (Lonza, Basel, Switzerland) vector or TrueORF gold vector coding for Myc-DDK-tagged ORF of human AIRE transcript variant AIRE-1 (OriGene Technologies, Rockville, Md) by using the jetPEI reagent (Polyplus Transfection, Illkirch, France). After 24 hours, fibroblasts were lysed in NP-40 lysis buffer (20 mmol/L Tris/HCl (pH 7.4], 150 mmol/L NaCl, 2 mmol/L EDTA, and 1% NP-40 (Sigma-Aldrich]) containing protease inhibitors for 30 minutes at 48C. Supernatants were collected after 10 minutes of centrifugation at 16,000g and 48C, and protein content was quantified with the mBCA quantification kit (Thermo Fisher Scientific Biosciences, Villebon sur Yvette, France). Protein extracts (50 μg) were analyzed by using Western blotting with anti-AIRE antibody (Abnova, Taipei, Taiwan), anti-rabbit IgG antibody conjugated to horseradish peroxidase (1:10,000, Sigma-Aldrich), and a BM Chemiluminescence Blotting Substrate Kit (Roche).

Measurement of gene expression in AIRE- transfected fibroblasts

Fibroblasts from patients or control subjects were cultured and transfected as above. After 24 hours, total RNA was extracted with TRIzol reagent, according to the manufacturer's instructions (Life Sciences). Quality and absence of genomic DNA contamination were assessed with a Bioanalyzer (Agilent, Massy, France). We used a high-capacity RNA-to-cDNA kit (Applied Biosystems) to generate cDNA for RT-PCR. PCR was carried out with a SybrGreen-based kit (FastStart Universal SYBR Green Master; Roche, Basel, Switzerland) on a StepOne plus instrument (Applied Biosystems). Primers were designed by using the

Roche Web site (Universal ProbeLibrary Assay Design Center) as follows: *IGFL1*, forward 5′-GGCTGCATCGTAGC TGTCTT-3′ and reverse 5′-GCATCAGGTAAGGAGTCATGG-3′; *Alox12*, forward 5′-CTGAAGATGGAGCCCAATG-3′ and reverse 5′-ACAGTGTTGGGGTTGGAGAG-3′; *PRMT3*, 5′-CAGGGTCGTGTTCTCTACGG-3′ and reverse 5′-TTTCCTTTCAAGGCTTCACCT-3′; *CCNH*, forward 5′-ATGATTACGTCTCAAAGAAATCCA-3′ and reverse 5′-CTACCAGGTCGTCATCAGTCC-3′; *CXCL10*, forward 5′-GAAAGCAGTTAGCAAGGAAAGGT- 39 and reverse 5′-GACATATACTCCATGTAGGGAAGTGA-3′; and *OAZ1*, forward 5′-GGATAAACCCAGCGCCAC-3′ and reverse 5′-TACAGCAGTG GAGGGAGACC-3′.

Detection of autoantibodies against CaSR

The immunoblotting method for detecting anti-CaSR autoantibodies is described elsewhere.[E6] Briefly, 20-mg samples of the *Escherichia coli*–expressed CaSR extracellular domain (amino acid residues 1-603; SWISS-PROT no. P41180) were separated by means of SDS-PAGE and transferred to nitrocellulose membranes. Membranes were used in standard immunoblotting experiments with patient or control sera (1:100 dilution), anti-human IgG antibody conjugated to horseradish peroxidase (1:2000 dilution, Sigma-Aldrich), and a BM Chemiluminescence Blotting Substrate Kit (Roche). In addition, anti-CaSR autoantibodies were detected in some patients' serum samples by using a CaSR immunoprecipitation assay, as detailed previously.[E7]

Detection of ANAs

The ANA detection method has been described elsewhere.[E8] Briefly, detection was performed by using an indirect immunofluorescence technique with HEp2 cells. Sera diluted at 1:160 were incubated on HEp2 cells (Bio-Rad, Marnes la Coquette, France) for 30 minutes at room temperature. After 3 washes in PBS, pH 7.4, the slides were incubated with a goat anti-human IgG ($F(ab')_2$) fluorescein isothiocyanate conjugated to fluorescein isothiocyanate (diluted at 1:100; Bio-Rad Laboratories, Hercules, Calif) for 30 minutes at room temperature. The slides were examined with an Olympus fluorescence microscope (Olympus, Center Valley, PA). A classical titration of each ANA positive at a titer of 1:160 was performed by means of serial 1-in-2 dilution until a dilution of 1:1280 was reached. A titer equal to or greater than 1:160 was interpreted as a positive result.

Statistical analyses

Differences in numbers of foci were analyzed by using the nonparametric Mann-Whitney *U* test (1-tailed; $P < .05$ was considered significant) in the GraphPad Prism program (GraphPad Software, La Jolla, Calif).

Study approval

The study was approved by the Medical Ethics Committee of Sud Est III (Lyon, France) and carried out in accordance with the Declaration of Helsinki principles. All patients provided written informed consent for inclusion of their details and samples in the study.

Acknowledgments

We thank the patients for their participation in this study. We also thank Nadia Plantier and ImmunID Technologies for providing the 3-dimensional immune repertoire analysis.

Supported by Hospices Civils de Lyon, Société Francaise de Rhumatologie, INSERM and ANR (ANR-14-CE14-0026-03) (to A.B.), as well as National Institutes of Health grant CA162804 (to D.J.C.), CPRIT RP110465 (to D.J.C.), and LYRIC grant INCa_4664 (to C.C.). T.W.'s laboratory is supported by European Research Council (ERC-Stg 281025), Institut National de la Santé et de la Recherche Médicale (INSERM), Centre National de la Recherche Scientifique (CNRS), Université Claude Bernard Lyon 1, ENS de Lyon. Y.J.C. acknowledges the European Research Council (GA 309449).

This study was supported by Hospices Civils de Lyon and INSERM, as well as National Institutes of Health (NIH) grant CA162804; CPRIT RP110465. G. I. Rice's institution has received funding from the European Research Council (GA309449: Fellowship to Y.J.C.). J. E. Walter and his institution have received funding from the NIH and National Institute of Allergy and Infectious Diseases (NIAID) (5K08AI103035). L. D. Notarangelo is employed at Boston Children's Hospital and is on the Board of Scientific Counselors of the NIAID and NIH, has received or has grants pending from the NIH and the March of Dimes, and receives royalties from UpToDate. M. Butte's institution has received funding from the NIH (R01 GM110482). H. Reumaux has received compensation for travel and other meeting-related expenses from the European League Against Rheumatism (EULAR). P. Cochat has received compensation for supplying expert testimony from Novartis, as well as for travel and other meeting-related expenses from Raptor Pharmaceuticals. M. van der Burg's institution received funding from ZonMW Vidi grant 91712323. Y. J. Crow has received funding from the European Research Council (GA 309449: Fellowship to Y.J.C.) and from the European Union's Seventh Framework Programme (FP7/2007-2013). J.-P. De Villartay's institution has received grants from INCa (PLBIO11-151) and Ligue National contre le Cancer. T. Walzer's institution has received funding from the European Research Council (ERC), and has received support for travel for this study or other purposes from ERC and his laboratory is supported by Agence Nationale de la Recherche, the European Research Council (ERC-Stg 281025), Institut National de la Santé et de la Recherche M'edicale (INSERM), Centre National de la Recherche Scientifique (CNRS), Université Claude Bernard Lyon 1, and ENS de Lyon. A. Belot's institution has received funding from the Institut national de la santé et de la recherche médicale, the French Society of Rheumatology, and Hospices Civils de Lyon; he has received compensation for delivering expert testimony from Pfizer, as well as compensation for travel and other meeting-related expenses from Novartis; and he has received or has grants pending from Advances in Neuroblastoma Research 2014.

Abbreviations used

AIRE	Autoimmune regulator
ANA	Antinuclear autoantibody
APECED	Autoimmune polyendocrinopathy, candidiasis, and ectodermal dystrophy
BAFF	B cell–activating factor
BCR	B-cell receptor
BMT	Bone marrow transplantation
CaSR	Calcium-sensing receptor
CID	Combined immunodeficiency
DCLRE1C	DNA cross-link repair 1C
DNA-PK	DNA-dependent protein kinase
DNA-PKcs	DNA-dependent protein kinase catalytic subunit
DSB	Double-strand break
LIG4	DNA ligase IV
mTEC	Medullary thymic epithelial cell

NK	Natural killer
OS	Omenn syndrome
PMA	Phorbol 12-myristate 13-acetate
RAG	Recombination-activating gene
SCID	Severe combined immunodeficiency

REFERENCES

1. Fischer A. Human primary immunodeficiency diseases. Immunity. 2007; 27:835–45. [PubMed: 18093537]
2. Felgentreff K, Perez-Becker R, Speckmann C, Schwarz K, Kalwak K, Markelj G, et al. Clinical and immunological manifestations of patients with atypical severe combined immunodeficiency. Clin Immunol. 2011; 141:73–82. [PubMed: 21664875]
3. Shearer WT, Dunn E, Notarangelo LD, Dvorak CC, Puck JM, Logan BR, et al. Establishing diagnostic criteria for severe combined immunodeficiency disease (SCID), leaky SCID, and Omenn syndrome: the Primary Immune Deficiency Treatment Consortium experience. J Allergy Clin Immunol. 2014; 133:1092–8. [PubMed: 24290292]
4. Villa A, Notarangelo LD, Roifman CM. Omenn syndrome: inflammation in leaky severe combined immunodeficiency. J Allergy Clin Immunol. 2008; 122:1082–6. [PubMed: 18992930]
5. De Villartay JP. V(D)J recombination deficiencies. Adv Exp Med Biol. 2009; 650:46–58. [PubMed: 19731800]
6. Schuetz C, Huck K, Gudowius S, Megahed M, Feyen O, Hubner B, et al. An immunodeficiency disease with RAG mutations and granulomas. N Engl J Med. 2008; 358:2030–8. [PubMed: 18463379]
7. Grunebaum E, Bates A, Roifman CM. Omenn syndrome is associated with mutations in DNA ligase IV. J Allergy Clin Immunol. 2008; 122:1219–20. [PubMed: 18845326]
8. Ege M, Ma Y, Manfras B, Kalwak K, Lu H, Lieber MR, et al. Omenn syndrome due to ARTEMIS mutations. Blood. 2005; 105:4179–86. [PubMed: 15731174]
9. Walter JE, Rucci F, Patrizi L, Recher M, Regenass S, Paganini T, et al. Expansion of immunoglobulin-secreting cells and defects in B cell tolerance in Rag-dependent immunodeficiency. J Exp Med. 2010; 207:1541–54. [PubMed: 20547827]
10. Anderson MS, Su MA. Aire and T cell Development. Curr Opin Immunol. 2011; 23:198–206. [PubMed: 21163636]
11. Mathis D, Benoist C. Aire. Annu Rev Immunol. 2009; 27:287–312. [PubMed: 19302042]
12. Gavalas NG, Kemp EH, Krohn KJ, Brown EM, Watson PF, Weetman AP. The calcium-sensing receptor is a target of autoantibodies in patients with autoimmune polyendocrine syndrome type 1. J Clin Endocrinol Metab. 2007; 92:2107–14. [PubMed: 17374709]
13. Irla M, Hugues S, Gill J, Nitta T, Hikosaka Y, Williams IR, et al. Autoantigen-specific interactions with CD4+ thymocytes control mature medullary thymic epithelial cell cellularity. Immunity. 2008; 29:451–63. [PubMed: 18799151]
14. Surh CD, Ernst B, Sprent J. Growth of epithelial cells in the thymic medulla is under the control of mature T cells. J Exp Med. 1992; 176:611–6. [PubMed: 1500862]
15. Poliani P, Vermi W, Facchetti F. Thymus microenvironment in human primary immunodeficiency diseases. Curr Opin Allergy Clin Immunol. 2009; 9:489–95. [PubMed: 19841578]
16. Poliani PL, Facchetti F, Ravanini M, Gennery AR, Villa A, Roifman CM, et al. Early defects in human T-cell development severely affect distribution and maturation of thymic stromal cells: possible implications for the pathophysiology of Omenn syndrome. Blood. 2009; 114:105–8. [PubMed: 19414857]

17. Cavadini P, Vermi W, Facchetti F, Fontana S, Nagafuchi S, Mazzolari E, et al. AIRE deficiency in thymus of 2 patients with Omenn syndrome. J Clin Invest. 2005; 115:728–32. [PubMed: 15696198]
18. Zhang S, Schlott B, GÖrlach M, Grosse F. DNA-dependent protein kinase (DNA-PK) phosphorylates nuclear DNA helicase II/RNA helicase A and hnRNP proteins in an RNA-dependent manner. Nucleic Acids Res. 2004; 32:1–10. [PubMed: 14704337]
19. Blunt T, Gell D, Fox M, Taccioli GE, Lehmann AR, Jackson SP, et al. Identification of a nonsense mutation in the carboxyl-terminal region of DNA-dependent protein kinase catalytic subunit in the SCID mouse. Proc Natl Acad Sci U S A. 1996; 93:10285–90. [PubMed: 8816792]
20. Gu Y, Seidl KJ, Rathbun GA, Zhu C, Manis JP, van der Stoep N, et al. Growth retardation and leaky SCID phenotype of Ku70-deficient mice. Immunity. 1997; 7:653–65. [PubMed: 9390689]
21. Abramson J, Giraud M, Benoist C, Mathis D. Aire's partners in the molecular control of immunological tolerance. Cell. 2010; 140:123–35. [PubMed: 20085707]
22. Woodbine L, Neal JA, Sasi NK, Shimada M, Deem K, Coleman H, et al. PRKDC mutations in a SCID patient with profound neurological abnormalities. J Clin Invest. 2013; 123:2969–80. [PubMed: 23722905]
23. Van der Burg M, Ijspeert H, Verkaik NS, Turul T, Wiegant WW, Morotomi-Yano K, et al. A DNA-PKcs mutation in a radiosensitive T-B- SCID patient inhibits Artemis activation and nonhomologous end-joining. J Clin Invest. 2009; 119:91–8. [PubMed: 19075392]
24. Torrado E, Cooper AM. IL-17 and Th17 cells in tuberculosis. Cytokine Growth Factor Rev. 2010; 21:455–62. [PubMed: 21075039]
25. Rice GI, del Toro Duany Y, Jenkinson EM, Forte GM, Anderson BH, Ariaudo G, et al. Gain-of-function mutations in IFIH1 cause a spectrum of human disease phenotypes associated with upregulated type I interferon signaling. Nat Genet. 2014; 46:503–9. [PubMed: 24686847]
26. De Saint-Basile G, Le Deist F, de Villartay JP, Cerf-Bensussan N, Journet O, Brousse N, et al. Restricted heterogeneity of T lymphocytes in combined immunodeficiency with hypereosinophilia (Omenn's syndrome). J Clin Invest. 1991; 87:1352–9. [PubMed: 2010548]
27. Schandené L, Ferster A, Mascart-Lemone F, Crusiaux A, Gérard C, Marchant A, et al. T helper type 2-like cells and therapeutic effects of interferon-gamma in combined immunodeficiency with hypereosinophilia (Omenn's syndrome). Eur J Immunol. 1993; 23:56–60. [PubMed: 8419187]
28. Miossec P. Interleukin-17 and Th17 cells: from adult to juvenile arthritis–now it is serious! Arthritis Rheum. 2011; 63:2168–71. [PubMed: 21380999]
29. HÖlttä V, Klemetti P, Sipponen T, Westerholm-Ormio M, Kociubinski G, Salo H, et al. IL-23/IL-17 immunity as a hallmark of Crohn's disease. Inflamm Bowel Dis. 2008; 14:1175–84. [PubMed: 18512248]
30. Ten Berge B, Paats MS, Bergen IM, van den Blink B, Hoogsteden HC, Lambrecht BN, et al. Increased IL-17A expression in granulomas and in circulating memory T cells in sarcoidosis. Rheumatology (Oxford). 2012; 51:37–46. [PubMed: 22075064]
31. Park J, Munagala I, Xu H, Blankenship D, Maffucci P, Chaussabel D, et al. Interferon signature in the blood in inflammatory common variable immune deficiency. PLoS One. 2013; 8:e74893. [PubMed: 24069364]
32. Scapini P, Hu Y, Chu CL, Migone TS, Defranco AL, Cassatella MA, et al. Myeloid cells, BAFF, and IFN-gamma establish an inflammatory loop that exacerbates autoimmunity in Lyn-deficient mice. J Exp Med. 2010; 207:1757–73. [PubMed: 20624892]
33. Sutherland AP, Ng LG, Fletcher CA, Shum B, Newton RA, Grey ST, et al. BAFF augments certain Th1-associated inflammatory responses. J Immunol. 2005; 174:5537–44. [PubMed: 15843552]
34. Romberg N, Chamberlain N, Saadoun D, Gentile M, Kinnunen T, Ng YS, et al. CVID-associated TACI mutations affect autoreactive B cell selection and activation. J Clin Invest. 2013; 123:4283–93. [PubMed: 24051380]
35. Andrès E, Limbach FX, Kurtz JE, Kurtz-Illig V, Schaeverbeke T, Pflumio F, et al. Primary humoral immunodeficiency (late-onset common variable immuno-deficiency) with antinuclear antibodies and selective immunoglobulin deficiency. Am J Med. 2001; 111:489–91. [PubMed: 11690576]

E1. Manuel M, Tredan O, Bachelot T, Clapisson G, Courtier A, Parmentier G, et al. Lymphopenia combined with low TCR diversity (divpenia) predicts poor overall survival in metastatic breast cancer patients. Oncoimmunology. 2012; 1:432–40. [PubMed: 22754761]

E2. Lim A, Baron V, Ferradini L, Bonneville M, Kourilsky P, Pannetier C. Combination of MHC-peptide multimer-based T cell sorting with the Immunoscope permits sensitive ex vivo quantitation and follow-up of human CD8+ T cell immune responses. J Immunol Methods. 2002; 261:177–94. [PubMed: 11861076]

E3. Pannetier C, Delassus S, Darche S, Saucier C, Kourilsky P. Quantitative titration of nucleic acids by enzymatic amplification reactions run to saturation. Nucleic Acids Res. 1993; 21:577–83. [PubMed: 8441670]

E4. Rubinstein S, Familletti PC, Pestka S. Convenient assay for interferons. J Virol. 1981; 37:755–8. [PubMed: 6163873]

E5. Familletti PC, Rubinstein S, Pestka S. A convenient and rapid cytopathic effect inhibition assay for interferon. Methods Enzymol. 1981; 78:387–94. [PubMed: 6173617]

E6. Mayer A, Ploix C, Orgiazzi J, Desbos A, Moreira A, Vidal H, et al. Calcium-sensing receptor autoantibodies are relevant markers of acquired hypoparathyroidism. J Clin Endocrinol Metab. 2004; 89:4484–8. [PubMed: 15356052]

E7. Gavalas NG, Kemp EH, Krohn KJ, Brown EM, Watson PF, Weetman AP. The calcium-sensing receptor is a target of autoantibodies in patients with autoimmune polyendocrine syndrome type 1. J Clin Endocrinol Metab. 2007; 92:2107–14. [PubMed: 17374709]

E8. Guyomard S, Salles G, Coudurier M, Rousset H, Coiffier B, Bienvenu J, et al. Prevalence and pattern of antinuclear autoantibodies in 347 patients with non-Hodgkin's lymphoma. Br J Haematol. 2003; 123:90–9. [PubMed: 14510947]

Key messages

- DNA-PKcs is a multifunctional protein involved in AIRE-dependent transcription in the thymus.
- *PRKDC* mutations can lead to a broad range of diseases, from SCIDs to milder immunodeficiency with granulomatous and autoimmune manifestations and positive anti-tissue autoantibody levels.

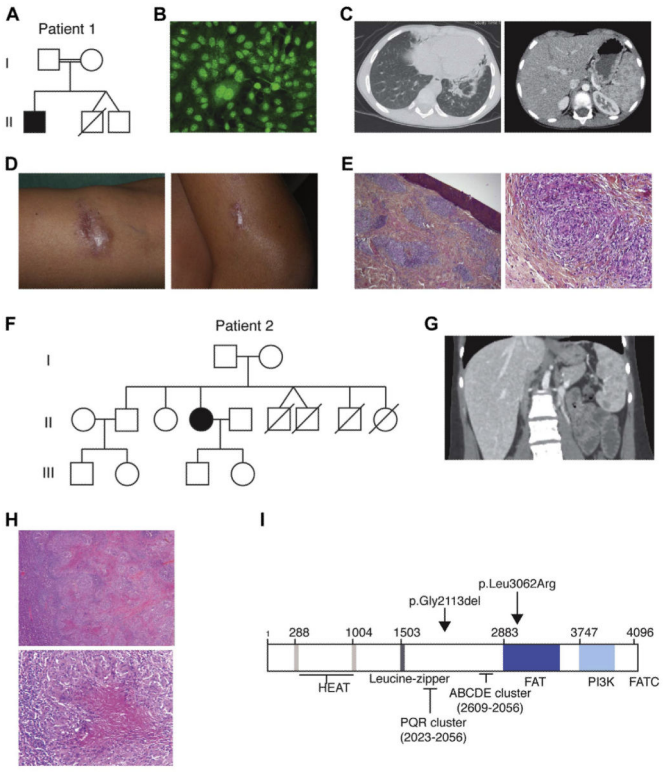

FIG. 1.

Clinical features of patients with *PRKDC* mutations. Pt1: **A**, family tree; **B**, positive antinuclear antibody levels; **C**, computed tomographic scan showing nodular lung lesions with infiltrate (*left panel*) and spleen granulomatous lesions (*right panel*); **D**, skin granulomatous lesion of the limb (*left panel*) and elbow (right panel); and **E**, epithelioid noncaseating granulomas from skin biopsy specimens. Pt 2: **F**, family tree; **G**, hepatomegaly with splenic granulomatosis (computed tomographic scan); **H**, caseating granulomas from spleen biopsy specimens; and **I**, schematic representation of the DNA-PKcs protein and the mutations identified in Pt1 and Pt2.

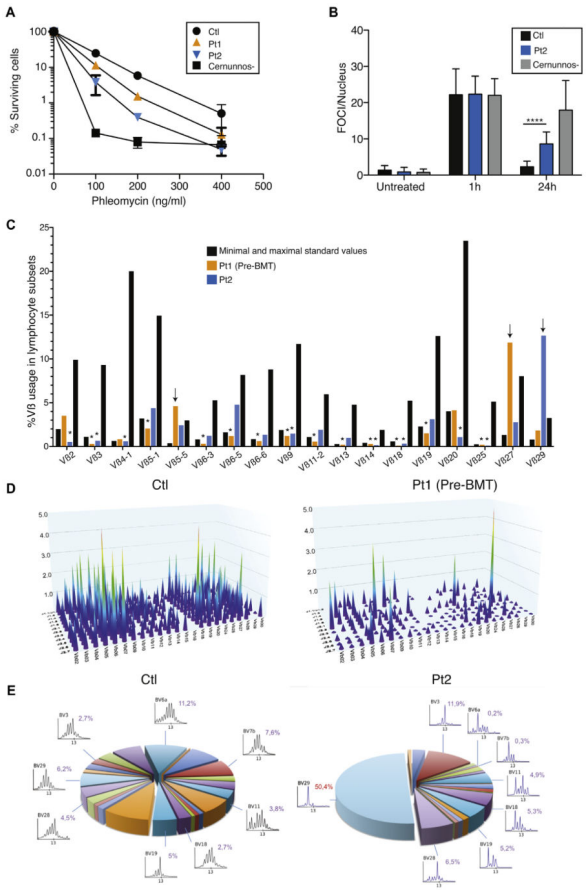

FIG. 2.

DSB repair defect and T-cell receptor oligoclonal repertoire. **A**, Clonogenic survival assays in fibroblasts from a control subject, a Cernunnos-deficient subject, Pt1, and Pt2. **B**, Numbers of γ-53BP1 foci *(FOCI)*/nucleus after irradiation in fibroblasts from a control subject, Pt2, and a Cernunnos-deficient subject. ****$P < .0001$. **C**, Quantitative analysis of Vβ distribution in $CD3^+$ T cells. Vβ underrepresentation (*asterisks*) or overrepresentation (*arrows*). **D**, Three-dimensional graph of immune combinatorial diversity in Pt1. *E*, Immunoscope of Vβ repertoire for the control subject and Pt2.

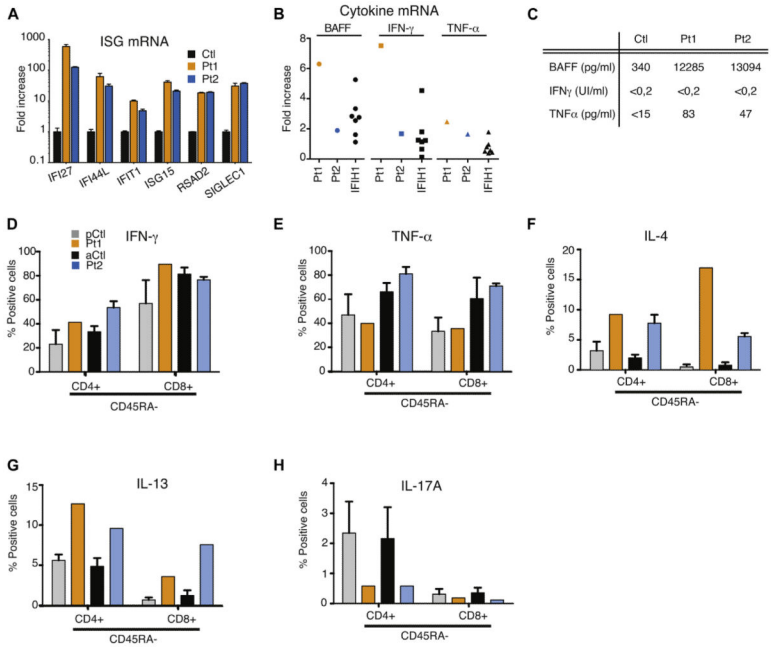

FIG. 3.

Cytokine expression in whole blood and on activation in T cells. **A** and **B**, RT-PCR of a panel of 6 interferon-stimulated genes (mean ± SD; Fig 3, A) and RT-PCR of a panel of 3 cytokines (Fig 3, *B*) in whole blood. **C**, BAFF, IFN-γ, and TNF-α measurements in sera of control subjects and Pt1 and Pt2. **D-H**, Cytokine expression in both CD4 and CD8 positive and CD45RA negative T cells as measured by using fluorescence-activated cell sorting in pediatric or adult control subjects (*pCtl* or *aCtl*, respectively) and Pt1 and Pt2.

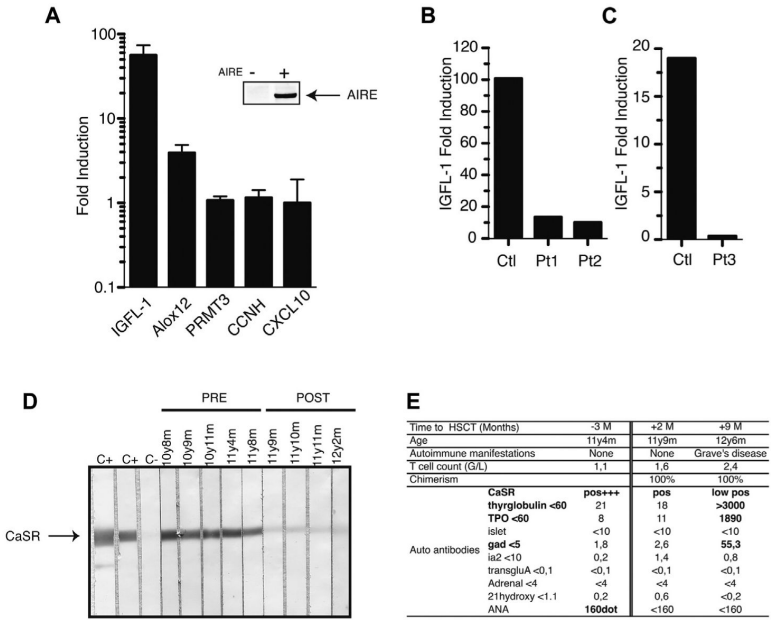

Time to HSCT (Months)		-3 M	+2 M	+9 M
Age		11y4m	11y9m	12y6m
Autoimmune manifestations		None	None	Grave's disease
T cell count (G/L)		1,1	1,6	2,4
Chimerism			100%	100%
Auto antibodies	**CaSR**	**pos+++**	**pos**	**low pos**
	thyrglobulin <60	21	18	**>3000**
	TPO <60	8	11	**1890**
	islet	<10	<10	<10
	gad <5	1,8	2,6	**55,3**
	ia2 <10	0,2	1,4	0,8
	transgluA <0,1	<0,1	<0,1	<0,1
	Adrenal <4	<4	<4	<4
	21hydroxy <1.1	0,2	0,6	<0,2
	ANA	**160dot**	<160	<160

FIG. 4.

PRKDC mutations prevent AIRE-dependent IGFL-1 expression. **A**, RT-PCR analysis of 5 transcripts after AIRE transfection in control fibroblasts. **B**, AIRE-dependent IGFL-1 expression in Pt1 and Pt2 or in the previously reported *PRKDC* mutant with SCID (Pt3). **C** and **D**, Detection of anti-CaSR autoantibodies in positive and negative control sera and Pt1's serum. **E**, Autoimmune markers in Pt1 before and after BMT.

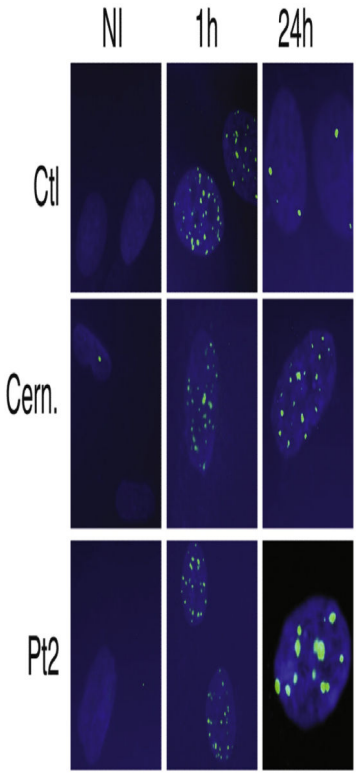

FIG E1.
53BP1 foci after X-irradiation of Pt2's fibroblasts. Time points were 1 and 24 hours.

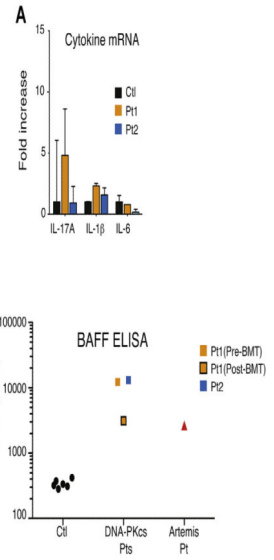

C

	%CD45RA-CD39+	S.D.	%CD45RA+CD39+	S.D.
pCtl	34.05	25.4	6.4	3.2
Pt1	96.8		0.8	
aCtl	35.9	16.1	6.7	3.7
Pt2	89.2		0.06	

FIG E2.

A, Quantitative RT-PCR of a panel of 3 cytokines in whole blood measured in Pt1 (before BMT) and Pt2 and 29 control subjects (mean 6 SD). **B**, BAFF measurement in sera of Pt1 (before and after BMT) and Pt2, one Artemis-deficient patient, and 6 control subjects by using ELISA. **C**, CD39 expression in regulatory T cells ($CD4^+CD25^+CD127^{low}$) in Pt1 (before BMT) and Pt2 compared with that in age-matched control subjects. *pCtl*, Pediatric control subject; *aCtl*, adult control subject.

TABLE I

Clinicobiological assessment of Pt1 and Pt2

	Patient 1 (before BMT)						Patient 2					
	6 y	**Normal values/µL (%)**	**8 y**	**10 y**	**11 y**	**Normal values/µL (%)**	**14 y**	**15 y**	**Normal values/µL**	**18 y**	**20 y**	**Normal values/µL**
Lymphocyte count/µL (%)	7324 (21)	2100-6450 (33-62)	774 (11)	1264 (18)	668 (13)	1440-5340 (29-56)	699 (15)	467 (12)	1400-3300	890 (32)	637 (14)	1000-4000
T-cell population/µL (%)												
$CD3^+$ cells	3589 (49)	1350-3900 (56-77)	387 (50)	670 (53)	334 (50)	1060-3370 (59-79)	433 (62)	289 (62)	1000-2200	623 (70)	376 (59)	700-2100
$CD3^+CD4^+$ cells	1245 (17)	740-2450 (27-49)	186 (24)	265 (21)	154 (23)	420-1930 (29-50)	269 (38)	165 (35)	530-1300	380 (42)	278 (44)	530-1300
$CD3^+CD8^+$ cells	1978 (27)	500-1610 (19-34)	194 (25)	392 (31)	180 (27)	410-138 (20-34)	91 (13)	90 (19)	390-920	168 (19)	49 (7)	330-920
Naive CD4 T cells ($CD4^+CD45RA^+$)	50 (4)	100-800 (66-77)	2 (1)	5 (2)	3 (2)	100-800 (55-67)	0	0	23-770	0	4 (1)	23-770
Memory CD4 T cells ($CD4^+CD45RO^+$)	1145 (92)	150-850 (NA)	171 (92)	252 (95)	137 (89)	150-850	269 (62)	182 (63)	240-700	423 (68)	263 (70)	240-700
Double-negative $CD3^+CD4^-CD8^-$ cells				1 (0.2)		9-78 (0.3-1.8)	17 (2)	14 (3)	9-78 (0.3-1.8)	19 (3)	56 (9)	7-74 (0.3-1.8)
Regulatory $CD3^+$ $CD25^+CD127^-$ cells				9 (3.4)	7 (4.8)	44-60 (4-10)						
TCRαβ cells					311 (93.1)	150-850 (80-98)						
TCRγσ cells					22 (6.5)	20-350						
Natural killer ($CD16^+CD56^+$ $CD3^-$) cells/µL (%)	3442 (47)	150-800 (6-19)	364 (47)	569 (45)	307 (46)	145-600 (6-21)	231 (33)	149 (32)	70-480	196 (22)	229 (36)	90-600
Dendritic cells					0.73	0.624-0.853					0.75	0.624-0.853
Monocytes												
Classical monocytes ($CD14^+CD16^-$)					3.64	472-780					1.44	472-780

	Patient 1 (before BMT)						Patient 2					
	6 y	**Normal values/μL (%)**	**8 y**	**10 y**	**11 y**	**Normal values/μL (%)**	**14 y**	**15 y**	**Normal values/μL**	**18 y**	**20 y**	**Normal values/μL**
Inflammatory monocytes ($CD14^+CD16^+$)					828.61	18-44					187.19	18-44
Nonclassical monocytes ($CD14^-CD16^+$)					88.19	15-39					35.08	15-39
B cells/βL (%)												
$CD19^+$	147 (2)	370-1570 (15-34)	8 (1)	13 (1)	7 (1)	230-1130 (10-27)	0	0	110-570			
Immunoglobulin (g/L)												
IgG				14.6	14.1	6.55-12.17					22	6.55-12.17
IgG_1				8.8	11.5	4.23-10.6						
IgG_2				<0.02	0.2	0.76-3.55						
IgG_3				1.159	1.131	0.17-1.73						
IgG_4				<0.003	<0.003	0.016-1.15						
IgA				<0.06	<0.06	0.51-1.63					<0.06	0.75-2.38
IgM				1.29	1.44	0.57-1.62					0.88	0.71-2.02
IgE					$<4.88 \times 10^{-6}$	$<366 \times 10^{-6}$					$<4.88 \times 10^{-6}$	$<366 \times 10^{-6}$

NA, Not applicable; *TCR*, T-cell receptor.

TABLE II

Anti-CaSR assessment in patients with V(D)J recombination deficiency

Patient	Mutation	Clinical history	Serum related to HSCT	Age at time of sample	CaSR antibody
Pt1	*PRKDC* p.Leu3062Arg; p.Leu3062Arg	Arthritis, skin granuloma, recurrent infections	Before After		Pos (46.4) Pos (3.26)
Pt2	PRKDC p.Leu3062Arg; p.Leu3062Arg	Arthritis, spleen granuloma, recurrent infections	Before		Pos (28.1)
Artemis	*DCLRE1C* p.Leu70del; p.0 (del exons 1–4)	No severe infection, cutaneous granuloma	Before	<6 y	Neg
RAG case 1	*RAG1* p.Arg474Cys; p.Lys983AsnfsX9	Autoimmune cytopenia, severe infections	Before After	2 y >29 mo	Neg Neg
RAG case 2	*RAG1* p.Arg474Cys; p.Lys983Asn	Autoimmune cytopenia, severe infections	Before	>8 y	Neg
RAG case 3	*RAG1* p.Arg841Gln; p.Phe974Leu	Idiopathic T-cell lymphopenia, sister with severe autoimmunity	Before	<3 mo	Neg
RAG case 4	*RAG1* p.His612Arg; pHis612Arg	Evans syndrome, skin granuloma, splenomegaly, severe infections	After	10 y	Neg
RAG case 5	*RAG1* p.Arg314Trp; p.Arg507Trp/Arg737His	Skin granuloma, EBV lymphoma, no severe infections	Before	<6 y	Neg
RAG case 6	*RAG2* p.Phe62Le; p.Phe62Leu	Autoantibodies, T-cell lymphopenia, severe infections	Before	29 y	Neg